RADIATIVE TRANSFER MODELING OF ILMENITE IN LUNAR BASALTS, PHYSICAL MIXTURES, AND IMPLICATIONS FOR MAPPING OF TITANIUM ON THE MOON.

K.M. Robertson[1], S. Li[2]., R.E. Milliken[1], C.M. Pieters[1] and P. Isaacson[1] Dept. of Earth, Environmental and Planetary Sciences, Brown University, Providence, RI, 02912, [2]Hawaii Institute of Geophysics and Planetology, University of Hawaii, Honolulu, HI.

Introduction: Fe-Ti oxides observed in returned lunar samples have proven to be useful phases for helping to constrain formation conditions of mare basalts and variations in their parent magmas [1]. As such, mapping the distribution and ilmenite content of high-Ti basalts across the lunar surface is a goal that requires use of remote sensing methods such as reflectance spectroscopy. However, limited sampling of these lithologies and complex spectral properties associated with the presence of Fe-Ti oxides (ilmenite) has made this a challenge.

Empirical correlations between TiO_2 content and spectral slope [2,3] across the UV-VIS wavelength range have been observed, but resulting estimates of TiO_2 can have relative uncertainties >50% [4]. This raises the question as to whether or not spectral radiative transfer models (RTMs) may yield better results, and Hapke's RTM [5] provides a means for quantitative un-mixing of spectra acquired for airless bodies such as the Moon [6]. However, there remain significant issues related to the quantification of strongly absorbing phases such as Fe-Ti oxides when mixed with silicates, as is the case for the lunar surface.

Reflectance spectra of ilmenite ($FeTiO_3$) exhibit complex spectral properties that include λ dependent opacity [7], highly variable albedo across the VIS-NIR λ range [8], and significant spectral variations due to sample texture [9]**.** These and other factors complicate the derivation of ilmenite optical constants that are the desired input for RTMs.

In this study we apply a Hapke radiative transfer model to laboratory spectra of a suite of lunar high-Ti basalts of known ilmenite content and synthetic ilmenite - pyroxene mixtures to better understand and reconcile how the spectral properties of ilmenite-bearing materials are affected by some of these factors. We then discuss the viability of quantifying ilmenite in high-Ti basalts on the moon using VIS-NIR spectroscopy.

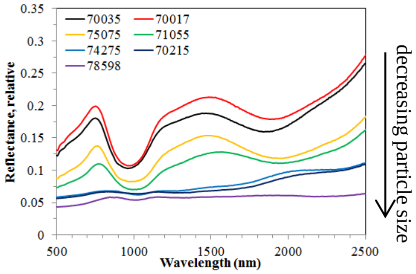

Figure 1. Comparison of BDR spectra for the suite of lunar basalt samples arranged from coarsest to finest ilmenite particle size. A distinct change in the spectral properties (albedo, slope, pyroxene absorptions) is observed with decreasing ilmenite particle size.

Methods: A suite of seven high-Ti lunar basalts were selected in order to understand the textural systematics of ilmenite in natural lunar samples. This suite of samples was chosen because the basalts have similar modal abundances, including ilmenite, but vary in terms of ilmenite particle size (~150 µm to < 20 µm). Prepared thin sections were mapped using an electron microprobe to obtain modal mineralogy and textural information (e.g., ilmenite grain size). Slabs corresponding to the thin sections were ground and sieved to large (>125 µm) and then small (<45 µm) size fractions for spectral measurements. Independent ilmenite-pyroxene physical mixtures were made to test the use of optical constants in quantifying ilmenite abundance and to assess the effect of ilmenite particle size in a more controlled setting. A synthetic pure ilmenite (100% Fe) sample (Alfa Aesar) and a Tanzanian enstatite were ground and wet sieved to four particle sizes (20-38 µm, 38-45 µm, 63-75 µm, 75-125 µm). The coarse ilmenite (75-125 µm) and small ilmenite (20-38 µm) were mixed (5 wt% increments up to 25 wt%) with all 4 size fractions of enstatite, producing a suite of 'coarse-' and 'small-grained' ilmenite mixtures. Reflectance spectra for all samples were measured once with the bi-directional spectrometer in RELAB at Brown University and 8 times on an ASD FieldSpec3 spectroradiometer using similar geometries (i=30º, e=0º, g=30º).

The overall parameterization of the Hapke model used in this study is the same as that of [10], where the model inputs are the measured reflectance data, viewing geometry (i, e, g), mineral densities, and endmember optical constants (or single scattering albedo, SSA, derived from the Hapke model). For the binary mixtures, the model used endmember optical constants calculated from the pure mineral spectra. For the lunar samples we used SSA of mineral endmembers to avoid errors due to large uncertainties in the optical constants of lunar ilmenite. The lunar basalt samples vary in ilmenite and

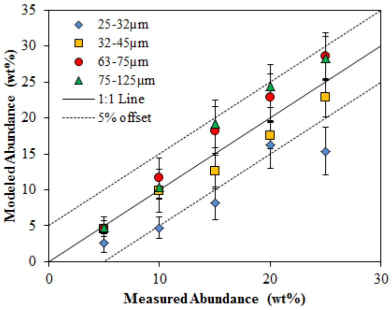

Figure 2. Modeled abundance values for the binary mixtures of coarse ilmenite with the different pyroxene particle sizes.

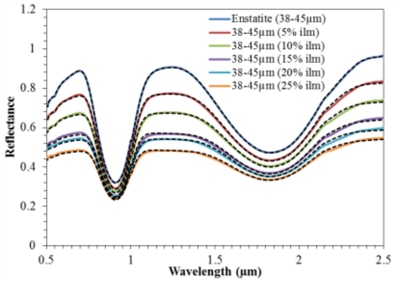

Figure 3. Modeled (black stippled line) vs measured spectra for the coarse imenite (75-125 µm) – pyroxene (38-45 µm) mixtures.

pyroxene composition; therefore multiple endmembers for each phase were required in the model to better represent the bulk basaltic compositions. Endmembers included lunar mineral separates (ilmenite/plag/augite/pigeonite) from the Lunar Rock and Mineral Characterization Consortium [8], 13 pyroxenes (synthetic and meteorite), and the alfa aesar ilmenite.

Results: The Hapke un-mixing results for the laboratory ilmenite mixtures are promising for all size fractions when using the optical constants calculated for the individual sieve size ranges. The modeled modal abundances for coarse ilmenite mixed with the 4 different size ranges of pyroxene are reported in Fig. 2. The average ilmenite abundance across all 8 measurements is within 5% of the measured values, but large variations are observed between measurements. The variations are not systematic and likely due to 1) preferential settling of coarser grains and/or 2) clustering of finer grained particles within the voids between larger particles during sample preparation. Spectral fits (Fig.3) are robust for all mixtures (RMS~10^{-5}), indicating the optical constants account for all major spectral properties.

In contrast, ilmenite particle size poses a significant issue when modeling spectra of the lunar basalts. Fine and coarse-grained ilmenite samples exhibit markedly different spectral properties (Fig. 1) that must be dealt with in the Hapke model. Modal abundance values (Fig.4) of ilmenite and pyroxene are quite close to the electron microprobe values, but plagioclase appears to be poorly constrained, even though spectral fits are robust (Fig.5). Results for samples with coarser ilmenite were consistently better, likely because the ilmenite endmember used in the model was derived from sample 70035 (coarse ilmenite). The model consistently chose the lunar ilmenite as opposed to the synthetic ilmenite since the slopes at the longer wavelengths were more comparable. It is evident by some of the misfits in the modeled spectra that there are still some issues with the pyroxene and ilmenite endmember compositions and/or physical form. This suite of lunar basalts has a range of Mg substitution (2-8%) in the ilmenite phase, which has significant effects on NIR spectral slopes [11].

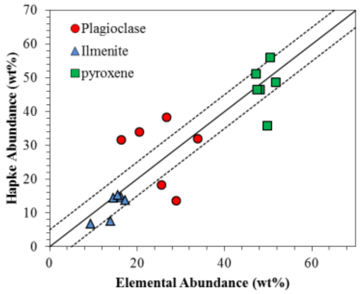

Figure 4. Modeled abundance values of the lunar basalts using SSA are compared with measured from the microprobe. There is good agreement for both ilm and pyx, however plagioclase is poorly constrained.

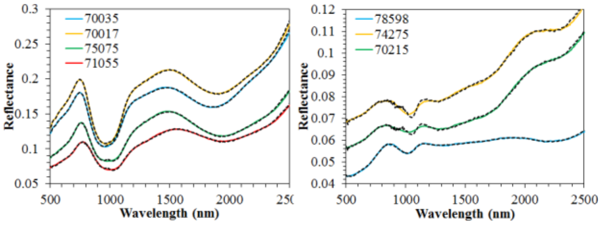

Figure 5. Modeled (black stippled line) vs measured spectra for the coarsely powdered (>125µm) lunar basalt suite. The spectral fits are quite good overall with RMS errors ~10^{-4}.

Conclusions: It is observed that fine-grained ilmenite in lunar basalts causes significant suppression of silicate absorption features, reduced albedo and a ‘red’ spectral slope at longer wavelengths compared with coarse-grained ilmenite in samples with similar modal value. Similar spectral trends are not as evident for synthetic mixtures with a limited range of sizes of ilmenite. The nonlinear spectral mixing behavior of ilmenite in the basalts is likely controlled by the intimate grain-on-grain boundaries of ilmenite with adjacent silicates.

The Hapke model is able to reproduce spectral variations in the lunar basalts when using SSA as opposed to optical constants, and modeled abundance values for pyroxene and ilmenite are similar to independently measured values. Residuals observed in the model fits can be attributed to minor variations in ilmenite/pyroxene compositions, which can likely be remedied by including additional endmembers.

Future work will include 1) expanding the endmember library by synthesizing ilmenite phases with variable Fe contents (90-99%) 2) deriving accurate optical constants for lunar ilmenite 3) focus on <20µm and observed grain-grain relations seen in the thin sections.

Acknowledgments: The authors acknowledge the support of NASA SSW grant NNS15AR68G.

References: [1] Neal and Taylor, (1992) *GCA* 79. [2] Gillis et al., (2003) *JGR*. 108b. [3] Lucey et al., (2000) *JGR*. 105. [4] Gillis-Davis et al., (2006) *GCA.70.* [5] Hapke, B., (2005) *Cambridge university press.* [6] Mustard, J.F. and C.M. Pieters, *JGR 94*. [7] Riner et al., (2009) *GRL.36.* [8] Isaacson et al., (2011) *Meteorit. Planet. Sci.* 46. [9] Robertson et al., (2017) *LPSC abstract #2127*. [10] Li and Li, (2011) *JGR*. E09001 [11] Tokle et al., (2018) *LPSC abstract.*